

IDA

INSTITUTE FOR DEFENSE ANALYSES

Very High Frequency (VHF) and Ultrahigh Frequency (UHF) Band Sky Noise Estimates From Analysis of 34.5 MHz and 408 MHz Sky Surveys

J. F. Heagy
J. Iams
J. M. Ralston

April 1998

Approved for public release;
distribution unlimited.

IDA Paper P-3395

Log: H 98-001156

19980811 147

This work was conducted under contract DASW01 94 C 0054, DARPA Assignment A-155, for the Defense Advanced Research Projects Agency/ISO. The publication of this IDA document does not indicate endorsement by the Department of Defense, nor should the contents be construed as reflecting the official position of that Agency.

© 1998 Institute for Defense Analyses, 1801 N. Beauregard Street, Alexandria, Virginia 22311-1772 • (703) 845-2000.

This material may be reproduced by or for the U.S. Government pursuant to the copyright license under the clause at DFARS 252.227-7013 (10/88).

INSTITUTE FOR DEFENSE ANALYSES

IDA Paper P-3395

**Very High Frequency (VHF) and Ultrahigh
Frequency (UHF) Band Sky Noise Estimates
From Analysis of 34.5 MHz and
408 MHz Sky Surveys**

J. F. Heagy
J. Iams
J. M. Ralston

PREFACE

This document was prepared by the Institute for Defense Analyses (IDA) under the task order entitled, "Counter Camouflage Concealment and Deception (CCC&D) Systems Studies." The work was supported by the Defense Advanced Research Projects Agency (DARPA). The authors would like to thank James Silk for valuable discussions during this work.

CONTENTS

A. Sky Surveys	1
B. Spectral Index and Cone-Averaging	3
C. Conclusion	8
Glossary	GL-1
References	R-1

FIGURES

1. All-Sky Temperature Survey at 408 MHz	2
2. All-Sky Temperature Survey at 34.5 MHz	3
3. Geometry of Cone-Averaging Procedure	6
4. Cone-Averaged Temperature at 408 MHz; $\beta_c = 30^\circ$	6
5. Cone-Averaged Temperature at 34.5 MHz; $\beta_c = 30^\circ$	7
6. Estimated Sky Temperatures Over the VHF and UHF Bands	8

TABLES

1. Mean Sky Temperatures and Standard Deviations Before and After Cone-Averaging	8
-------------------------------------------------------------------------------------------	---

VERY HIGH FREQUENCY (VHF) AND ULTRAHIGH FREQUENCY (UHF) BAND SKY NOISE ESTIMATES FROM ANALYSIS OF 34.5 MHz AND 408 MHz SKY SURVEYS

A. SKY SURVEYS

Several all-sky radio surveys exist. Of these, two in the frequency band of interest have been singled out for analysis. The first survey, at 408 MHz, was published in 1982 by Haslam, et al. (Ref. 1). This survey, which covers the entire celestial sphere at an angular resolution of $0.85^\circ \times 0.85^\circ$, is a compilation of data taken with four radio telescopes at various locations on Earth. The second survey, at 34.5 MHz, was published in 1990 by Dwarakanath and Shankar (Ref. 2). It covers declinations from -50° to 70° . Observations were made from a single radio telescope in Gauribidanur, India.

Both data sets are in the public domain and can be obtained in Flexible Image Transport System (FITS) format from the Skyview Virtual Observatory web site, <http://skyview.gsfc.nasa.gov>. This web site is an astronomical data repository maintained by the Goddard Space Flight Center (GSFC).

Radio FITS data are expressed in Kelvins (K). Let the measured brightness of a radio source with right ascension α , declination δ , and frequency ν be B . B has units of $\text{watts m}^{-2} \text{Hz}^{-1} \text{rad}^{-2}$. The temperature, T , associated with this measurement is found through the low frequency limit of the Planck blackbody distribution curve, namely, the Rayleigh-Jeans law (Ref. 3),

$$B = \frac{2\nu^2 kT}{c^2} = \frac{2kT}{\lambda^2} \quad , \quad (1)$$

where k is the Boltzmann constant.

Figures 1 and 2 show the temperature maps of the 408 and 34.5 MHz surveys. Temperature scales are given to the right of each image. Each image is expressed as a rectangular projection in Earth equatorial coordinates, with the usual astronomical convention that right ascension α increases to the left. The size of each image is 360×180 pixels ($1^\circ \times 1^\circ$ resolution). The galactic plane is the sinusoidal yellow region in each survey.

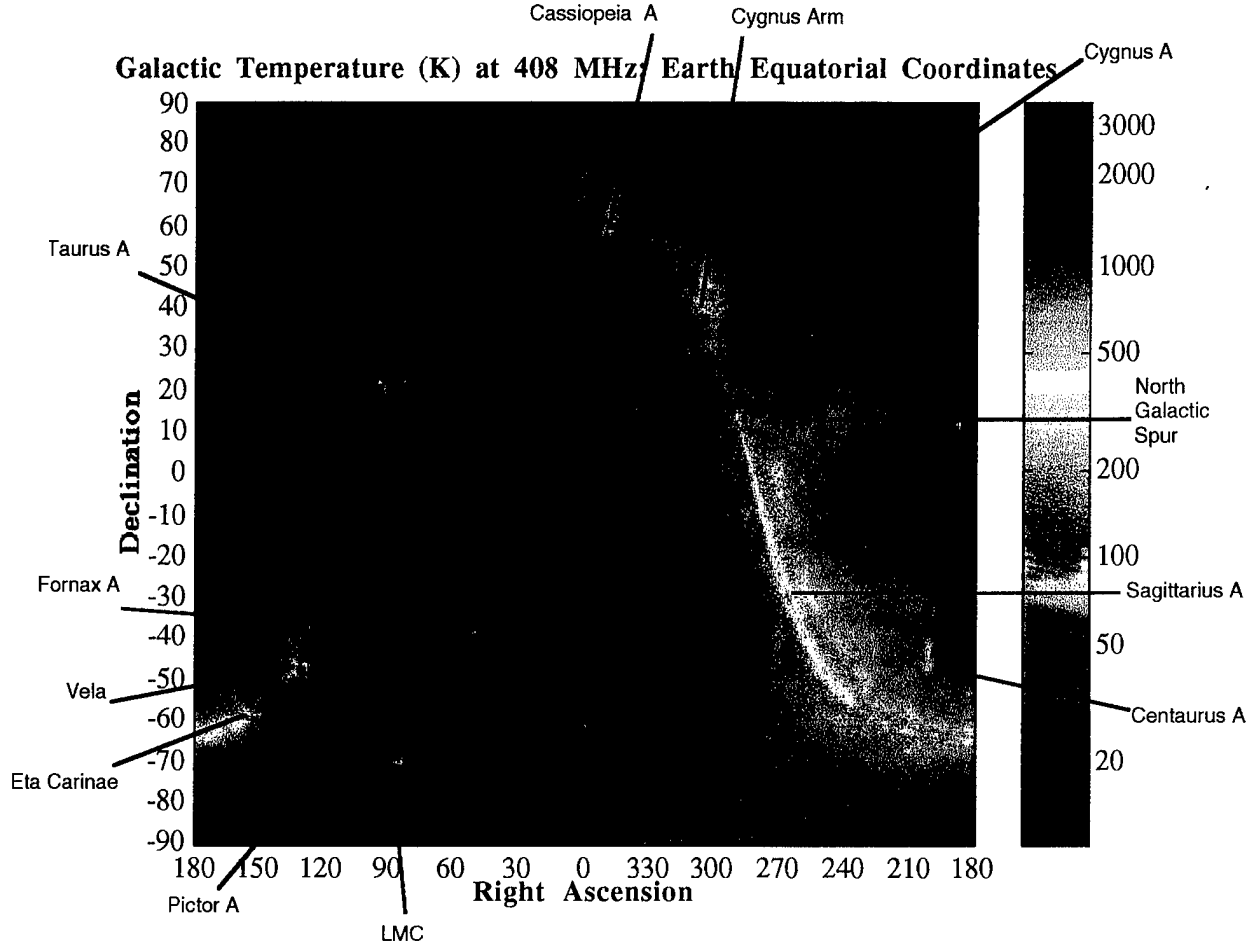


Figure 1. All-Sky Temperature Survey at 408 MHz

Prominent radio sources are identified in the 408 MHz survey. The brightest discrete source in each survey is the supernova remnant Cassiopeia A, which is located at $(350.29^\circ, 58.55^\circ)$. However, the brightness and extent of the galactic center (Sagittarius A) at $(265.52^\circ, -28.92^\circ)$ makes it the dominant radio noise source in the sky.

The raw 34.5 MHz data must be pre-processed, since it contains values of zero temperature outside the survey region (declinations above 70° and below -50°) and a few isolated zero and negative temperature values within the survey region. These values are presumably dropouts because of data acquisition difficulties. For convenience, the zero and negative values have been replaced with the spherically averaged temperature over the positive-valued survey region Ω_R ,

$$\langle T \rangle = \frac{1}{\Omega_R} \int_{\Omega_R} T(\alpha, \delta) d\Omega \quad , \quad (2)$$

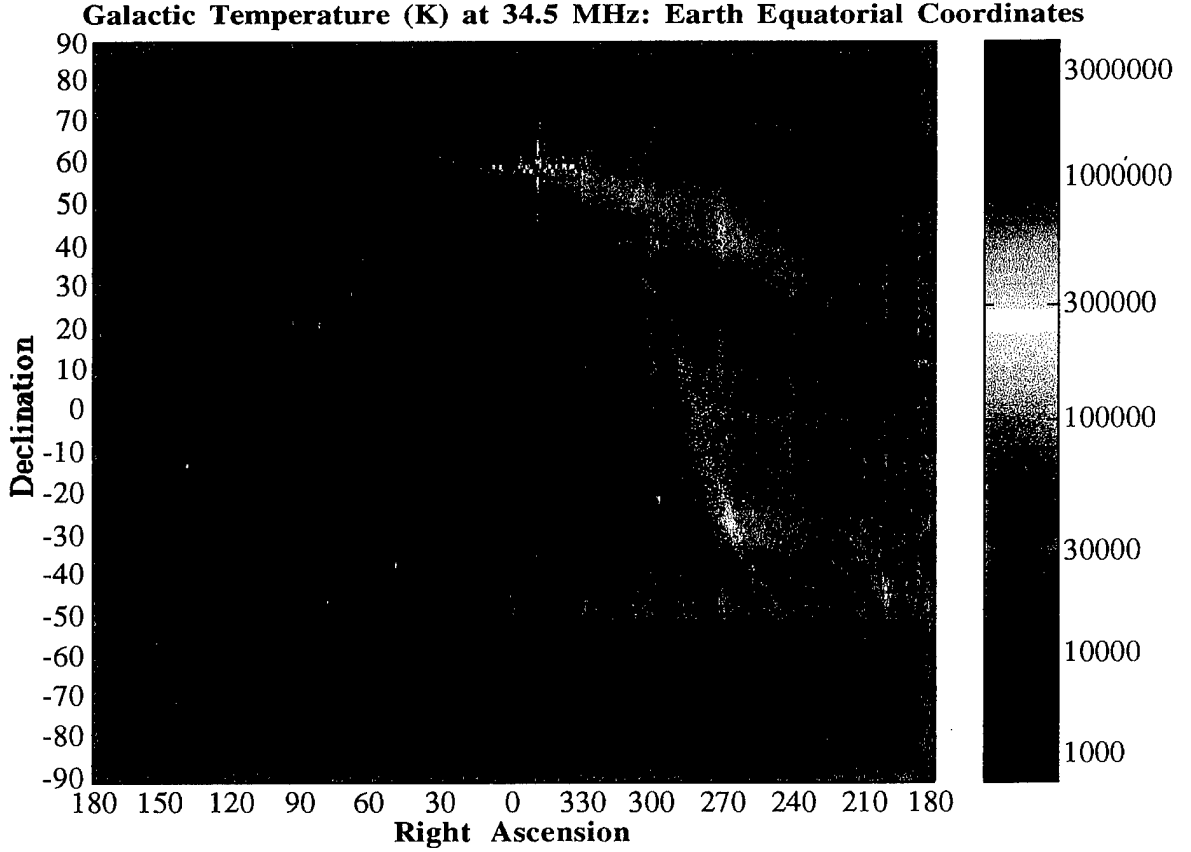


Figure 2. All-Sky Temperature Survey at 34.5 MHz

where $d\Omega = \cos\delta d\delta d\alpha$. The image shown in Figure 2 is constructed from the pre-processed 34.5 MHz data set.

B. SPECTRAL INDEX AND CONE-AVERAGING

Note the great difference in temperature scales between the two surveys. The average temperatures for each survey can be computed from Eq. (2) by allowing Ω_R to be the entire celestial sphere. The averages are $\langle T_{408} \rangle = 22.13$ K and $\langle T_{34.5} \rangle = 12,317$ K. The radio sky, therefore, does not behave as a blackbody whose temperature is constant for all frequencies. This is because strong radio emitters are generally nonthermal in nature. They are believed to be dominated by sources of synchrotron radiation (Ref. 3).

A temperature-frequency dependence of the form

$$T = a\nu^{-\eta} \quad , \quad (3)$$

where the exponent η is known as the temperature spectral index and a is a proportionality constant, is often assumed to hold for nonthermal radio sources. This relation has a solid theoretical justification for single synchrotron radiation sources (Ref. 3). Spectral indices are typically in the 2.4 to 2.7 range.

For the radars of interest, having an estimate of the spherically averaged sky temperature at frequencies in the 30 to 1,000 MHz range is desirable. This is done as follows. Assuming that the model [Eq. (3)] holds, the nominal spectral index η can be found from the spherically averaged temperatures computed previously:

$$\eta = \frac{\ln(\langle T_{34.5} \rangle / \langle T_{408} \rangle)}{\ln(408/34.5)} = 2.56 \quad (4)$$

The constant a is then found from Eq. (3) by using the average temperature at one of the two frequencies with $\eta = 2.56$. The result is $a = 1.06 \times 10^8$ in units where T is in Kelvins and ν is in MHz.

Note that other methods can be used to extract η and a . For example, η can be found by computing a spectral index for each pair of corresponding temperature values between the two sky surveys. The mean value provides an estimate of η . Carrying this out, one finds $\langle \eta \rangle = 2.57$, which differs only slightly from the result in Eq. (4). The parameter a can then be found self-consistently by computing the mean of the quantity $a = T \nu^{-\eta}$ for the data in both surveys. The result is $\langle a \rangle = 1.76 \times 10^8$. This result is considerably larger than the value of 1.06×10^8 , which was found with the first method. The reason for this difference is that the second method treats all temperatures with equal weighting, while the first method properly treats the spherical support of the data. Since our interest is in average temperatures over the desired frequency range, we rely on the first method to compute η and a .

It is possible to estimate the standard deviation in the temperature at each frequency and the uncertainties in the parameters η and a by using the following heuristic "bootstrap" procedure. First, the standard deviations at the measured frequencies are computed from the mean square temperature

$$\langle T^2 \rangle = \frac{1}{\Omega_R} \int T^2(\alpha, \delta) d\Omega \quad (5)$$

and the mean temperature [Eq. (2)] through the general relation

$$\sigma = \sqrt{\langle T^2 \rangle - \langle T \rangle^2} \quad (6)$$

The results are $\sigma_{34.5} = 19,055$ K and $\sigma_{408} = 35.65$ K.

Suppose surveys at several frequencies ν_i were available, with corresponding mean temperatures T_i and standard deviations σ_i . Then, the parameters η and a would be found by minimizing the chi-square statistic

$$\chi^2 = \sum_i \left(\frac{T_i - a \nu_i^{-\eta}}{\sigma_i} \right)^2 . \quad (7)$$

This would yield the best-fit parameters, η and a , and the uncertainties in these parameters, σ_η and σ_a . Knowledge of these uncertainties would allow one to compute temperature variances at other frequencies through the propagation of variance equation

$$\sigma_T^2 = \left(\frac{\partial T}{\partial a} \right)^2 \sigma_a^2 + \left(\frac{\partial T}{\partial \eta} \right)^2 \sigma_\eta^2 , \quad (8)$$

assuming no cross-correlations between η and a . Computing the partial derivatives from Eq. (3) and dividing both sides by T^2 leads to

$$\frac{\sigma_T^2}{T^2} = \frac{\sigma_a^2}{a^2} + (\ln \nu)^2 \sigma_\eta^2 . \quad (9)$$

Assuming this expression can be used for the two data points under consideration, the parameter uncertainties σ_η and σ_a can be computed from the known values of T and σ_T at 34.5 MHz and 480 MHz. The results are $\sigma_a = 1.60 \times 10^8$ and $\sigma_\eta = 0.09$.

A real radar “sees” a much smoother temperature profile than those shown in Figures 1 and 2. Consider a receiving antenna pointed directly away from Earth in some direction (α_c, δ_c) . The radar will generally have a receiving pattern that subtends a solid angle, $\Delta\Omega$, that is large compared to the $1^\circ \times 1^\circ$ resolution displayed in Figures 1 and 2. The received energy is effectively an average over the patch of sky contained within $\Delta\Omega$ centered at (α_c, δ_c) .

The temperature profile seen by a “typical” radar is simulated as follows. Assume the energy incident at the radar antenna emanates from a patch of sky contained within a cone in the direction (α_c, δ_c) , with cone angle β_c (see Figure 3). The cone-averaged sky temperature in the direction (α_c, δ_c) is given by the average temperature over the solid angle subtended by the cone:

$$T_{\text{cone}}(\alpha_c, \delta_c; \beta_c) = \frac{1}{\Delta\Omega} \int T(\alpha, \delta) K(\alpha - \alpha_c, \delta - \delta_c; \beta_c) d\Omega , \quad (10)$$

where the integration is carried out over the entire celestial sphere and the kernel K is unity for angles inside the cone and is zero elsewhere. Figures 4 and 5 show the smoothed temperature profiles at 408 MHz and 34.5 MHz for a cone angle $\beta_c = 30^\circ$.

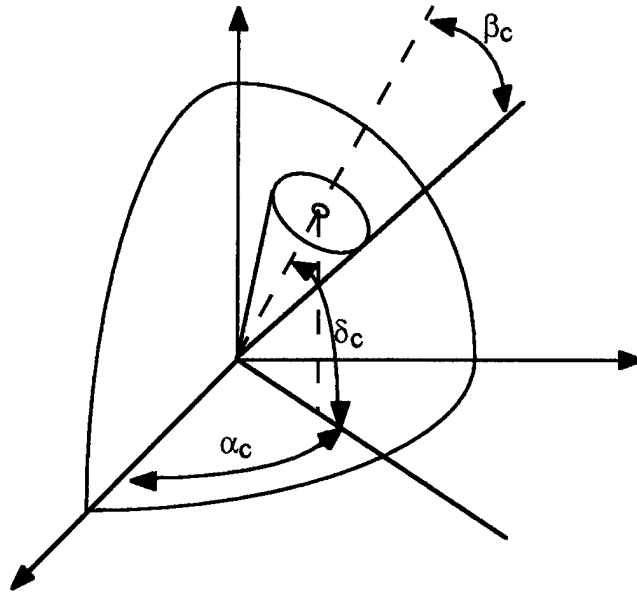


Figure 3. Geometry of Cone-Averaging Procedure

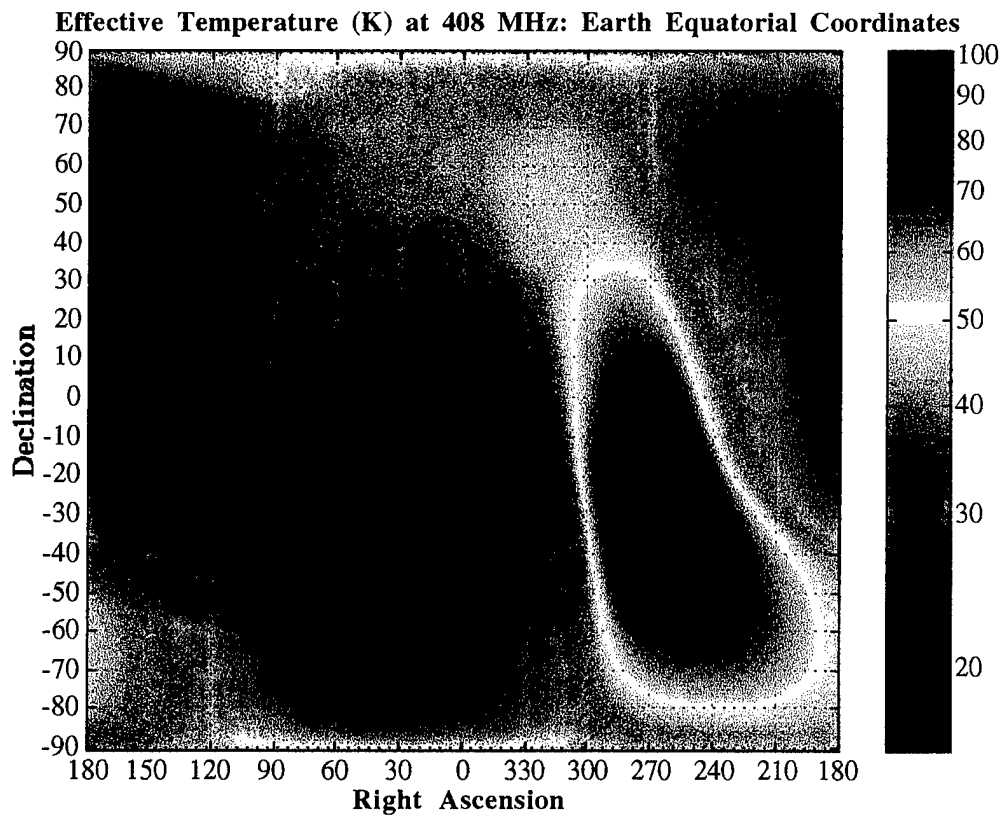


Figure 4. Cone-Averaged Temperature at 408 MHz; $\beta_c = 30^\circ$

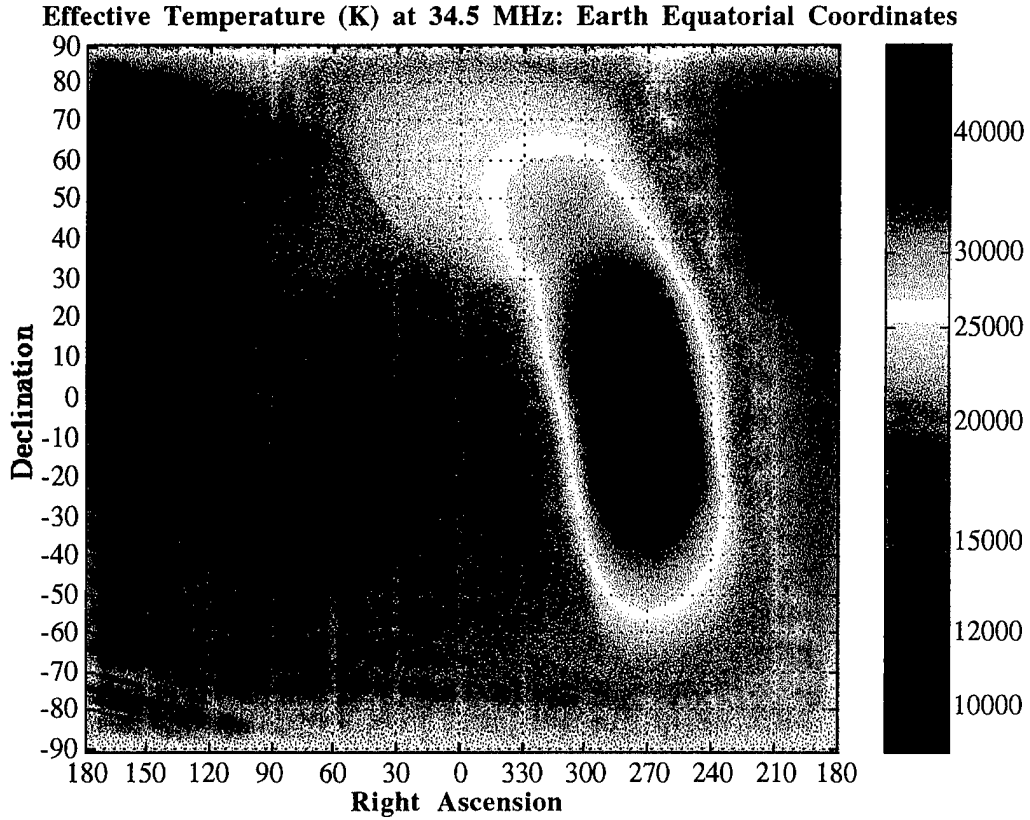


Figure 5. Cone-Averaged Temperature at 34.5 MHz; $\beta_c = 30^\circ$

The averaging operation heightens the similarities between the two spatial temperature distributions. The galactic center spreads its effects over a significant fraction of the southern hemisphere, while Cassiopeia A stands out prominently at northern latitudes.

As was done previously for the raw temperature data, the standard deviation for the cone-averaged data can be computed from Eqs. (2), (5), and (6). In principle, the average temperatures before and after cone-averaging should be the same since the integral [Eq. (10)] is “norm-preserving”; however, there are slight changes, presumably caused by errors in approximating the integral in Eq. (10) with a finite sum. Table 1 summarizes the averages and standard deviations before and after cone-averaging. Cone-averaging is seen to reduce the standard deviation significantly in each survey.

The bootstrap method discussed previously can also be used to estimate the parameter uncertainties and the temperature standard deviations for the cone-averaged data. Using the data in Table 1, one finds $\sigma_\eta = 0.09$ and $\sigma_a = 9.2 \times 10^7$ from Eq. (9).

Table 1. Mean Sky Temperatures and Standard Deviations Before and After Cone-Averaging

Data Set	$\langle T \rangle$ (K)	σ_T (K)
408 MHz (raw)	22.13	35.65
408 MHz (cone-averaged)	22.09	22.51
34.5 MHz (raw)	12317	19055
34.5 MHz (cone-averaged)	12295	11332

Our estimate of the sky temperature in the 30 to 1,000 MHz range is taken to be the spherically averaged mean temperature computed from Eq. (3) plus one sigma computed from Eq. (9), with the cone-averaged parameter uncertainties $\sigma_\eta = 0.09$ and $\sigma_a = 9.2 \times 10^7$ (Ref. 4). Figure 6 shows this temperature along with the mean temperature and the one sigma level for the raw data.

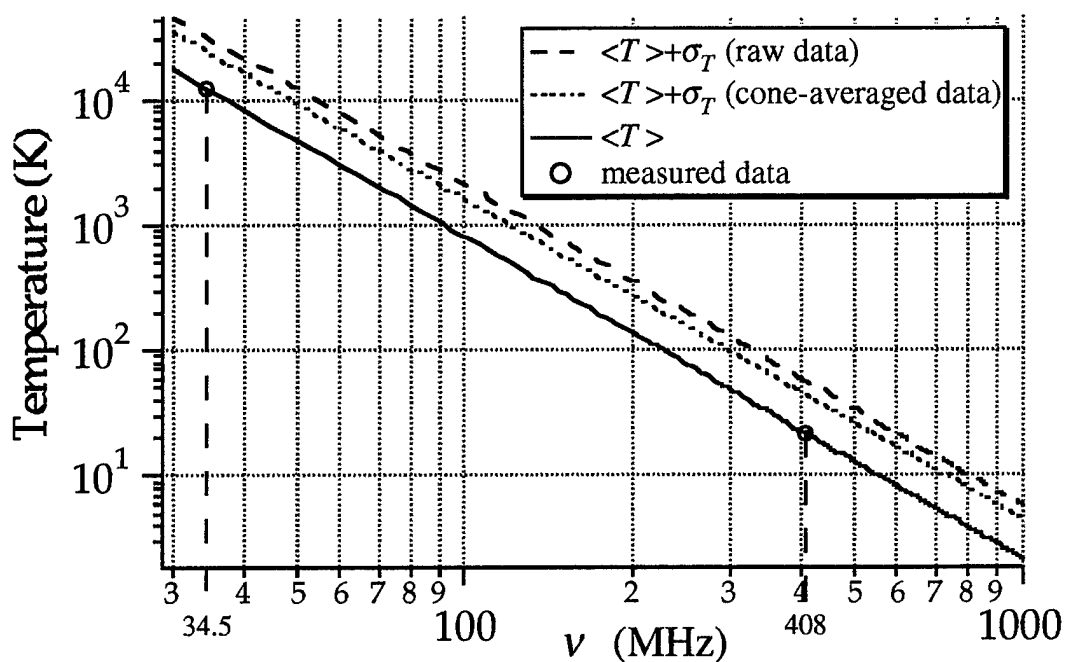


Figure 6. Estimated Sky Temperatures Over the VHF and UHF Bands

C. CONCLUSION

Analysis of radio sky surveys at 408 MHz and 34.5 MHz has furnished estimates of sky temperature throughout the VHF and UHF bands (30 to 1,000 MHz). This has

been accomplished through an empirical method that extends the fitted powerlaw temperature model to the entire frequency range of interest. Estimates of noise variance have also been made using a simple propagation of variance assumption. Results of this analysis are prerequisites for the evaluation of system noise temperatures in proposed radars (Ref. 4).

GLOSSARY

CCC&D	Counter Camouflage Concealment and Deception
DARPA	Defense Advanced Research Projects Agency
FITS	Flexible Image Transport System
GSFC	Goddard Space Flight Center
IDA	Institute for Defense Analysis
K	Kelvin
MHz	megahertz
UHF	ultrahigh frequency
VHF	very high frequency
www	World Wide Web

REFERENCES

1. C. G. T. Haslam, et al., "A 408 MHz All-Sky Continuum Survey. II. The Atlas of Contour Maps," *Astron. Astrophys. Suppl. Ser.*, Vol. 47, 1982, p. 1.
2. K. S. Dwarkanath and N. U. Shankar, "A Synthesis Map of the Sky at 34.5 MHz," *J. Astrophys. Astron.*, Vol. 11, 1990, p. 323.
3. John D. Kraus, *Radio Astronomy*, 2nd Ed., Cygnus-Quasar Books, Powell, Ohio, 1986.
4. J. Ralston, J. Heagy, and R. Sullivan, *Environmental Noise Effects on VHF/UHF UWB SAR*, IDA Memo, July 1997.

REPORT DOCUMENTATION PAGE

Form Approved
OMB No. 0704-0188

Public Reporting burden for this collection of information is estimated to average 1 hour per response, including the time for reviewing instructions, searching existing data sources, gathering and maintaining the data needed, and completing and reviewing the collection of information. Send comments regarding this burden estimate or any other aspect of this collection of information, including suggestions for reducing this burden, to Washington Headquarters Services, Directorate for Information Operations and Reports, 1215 Jefferson Davis Highway, Suite 1204, Arlington, VA 22202-4302, and to the Office of Management and Budget, Paperwork Reduction Project (0704-0188), Washington, DC 20503.

1. AGENCY USE ONLY (Leave blank)		2. REPORT DATE April 1998	3. REPORT TYPE AND DATES COVERED Final—July 1997–November 1997	
4. TITLE AND SUBTITLE Very High Frequency (VHF) and Ultrahigh Frequency (UHF) Band Sky Noise Estimates From Analysis of 34.5 MHz and 408 MHz Sky Surveys			5. FUNDING NUMBERS C—DASW01 94 C 0054 DARPA Task A-155	
6. AUTHOR(S) James F. Heagy, Joel Iams, James M. Ralston				
7. PERFORMING ORGANIZATION NAME(S) AND ADDRESS(ES) Institute for Defense Analyses 1801 N. Beauregard St. Alexandria, VA 22311-1772			8. PERFORMING ORGANIZATION REPORT NUMBER IDA Paper P-3395	
9. SPONSORING/MONITORING AGENCY NAME(S) AND ADDRESS(ES) DARPA/ISO 3701 N. Fairfax Drive Arlington, VA 22203-1714			10. SPONSORING/MONITORING AGENCY REPORT NUMBER	
11. SUPPLEMENTARY NOTES				
12a. DISTRIBUTION/AVAILABILITY STATEMENT Approved for Public Release—Distribution Unlimited			12b. DISTRIBUTION CODE	
13. ABSTRACT (Maximum 180 words) Ultrawideband (UWB) radars operating in the UHF and VHF frequency bands, 30–1,000 MHz, are subject to a variety of environmental noise sources (non-man-made sources). Chief among these are strong radio emitting astronomical sources, notably the center of the Milky Way galaxy and supernova remnants. Two recent radio sky surveys, one at 408 MHz and the other at 34.5 MHz, are analyzed to evaluate the impact of radio sky noise on the performance of UWB radars. To this end, sky temperatures are estimated throughout the 30–1,000 MHz range for a hypothetical radar with a 30° beam half-width. Effective temperatures are also estimated for evaluating system temperatures for a spot receiver operating in the 40–400 MHz band and a UWB synthetic aperture radar (SAR) operating in the 30–100 MHz band.				
14. SUBJECT TERMS radio noise, sky temperature, ultrawideband radar, synthetic aperture radar (SAR)			15. NUMBER OF PAGES 18	
			16. PRICE CODE	
17. SECURITY CLASSIFICATION OF REPORT UNCLASSIFIED	18. SECURITY CLASSIFICATION OF THIS PAGE UNCLASSIFIED	19. SECURITY CLASSIFICATION OF ABSTRACT UNCLASSIFIED	20. LIMITATION OF ABSTRACT SAR	